Modelling of progressive failure mechanism of mine pillars

Modelling of progressive failure mechanism of mine pillars

G Cammarata[1]*, D Elmo[2] and S Brasile[3]

[1]Bentley Systems Italia S.r.l., Milan, Italy
[2]University of British Columbia, NBK Institute of Mining Eng., Vancouver, Canada
[3]Plaxis B.V., a Bentley Systems company, Delft, The Netherlands

*Giuseppe Cammarata, e-mail: giuseppe.cammarata@bentley.com

Abstract. Rock fracturing process around underground openings is mainly a process of progressive slabbing with the generation of surface-parallel fractures in the initial stage, and shear failure is likely to occur in the final process. The difficulty of capturing this behaviour through conventional continuum modelling has led to the development of advanced constitutive laws for use in continuum models. Recently, an enhanced continuum constitutive approach to simulate strain-softening based on the Hoek-Brown failure criterion has been presented. This advanced Hoek-Brown model with Softening introduces a hyperbolic decay of the material properties affecting the post-peak response and the nonlinear dilation, thus enabling to investigate failure modes in the form of dilatant shear bands. Moreover, to restore the objectivity of the numerical solution during the development of strain localization phenomena, a viscous regularization technique has been implemented within the model. The performance of this constitutive model has been proved and, in this paper, further numerical computations are reported concerning the brittle failure process occurring in mine pillars, thus confirming the capability to capture failure mechanisms during excavation within a strain localization regime.

1. Introduction

The understanding and numerical modelling of the mechanical behaviour of rock masses at depth has a crucial role in the design of underground works where brittle failure resulting in spalling and rock bursting might occur.

Rock pillars are used in most underground mining methods, either temporary or permanent, to support the weight of overburden material between adjacent underground openings and thus to extract the ore safely. However, as mine depths increase, hard rock pillar failure becomes more critical due to the increase in in-situ stresses: progressive fracturing resulting in slabbing and spalling leads to loss of load-carrying capability. Hence, the prediction of rock pillar progressive failure behaviour becomes crucial for designing deep mining deployment systems. Besides the most generally accepted techniques for estimating pillar strength (defined as the ultimate load per unit area of a pillar) that use empirical and simplified methods, numerical methods provide a better alternative to understand and capture the brittle failure process of rock masses. Numerical simulations using both continuum, discontinuum and hybrid modelling approaches have, in fact, provided important contributions to the study of pillar behaviour in the context of progressive failure [e.g., 1, 2, 3, 4, 5, 6].

For simulating these failure phenomena, where induced fracturing plays a major role, discontinuum and hybrid continuum/discontinuum modelling approaches seem adequate and reliable. However, continuum models are still more commonly used than discontinuum/hybrid models. The latter are

generally more complex to use in practical rock engineering. In contrast, continuum modelling builds upon existing experience usually available in the technical community, which has led to constant developments and improvements in constitutive models for brittle failure [e.g., 7, 8, 9].

Recently, an enhanced continuum constitutive approach has been proposed [10], namely, the Hoek-Brown model with Softening (HBS). It includes a Hoek-Brown (HB) yield with a hyperbolic decrease of the material properties to simulate the degradation occurring in the transition between the peak and the corresponding residual behaviour in the brittle regime. The performances of this constitutive model have been investigated through numerical computations carried out with the finite element code PLAXIS [11] to simulate failure mechanisms characterized by dilatant shear bands [12].

This paper focuses on the simulation of the brittle failure process occurring in hard rock pillars using the HBS model. A summary of the main features of the model is first addressed (details of the mathematical framework and constitutive formulation are reported in [10] and [12]). Results showing the simulated progressive failure of different pillar width-to-height (*w*/*h*) ratios are then presented, confirming the model's capability to capture failure mechanisms within a strain localization regime.

2. Hoek-Brown with Softening model

In the HBS model, the yield criterion proposed by Jiang [13] is used as a basis to enrich the constitutive framework by implementing:

- a hyperbolic softening rule to consider the material degradation in the post-peak regime;
- a non-associated plastic flow characterized by nonlinear dilation;
- a tension cut-off for the tensile regime;
- a viscous regularization technique aimed to restore the objectivity of the numerical solution.

The resulting yield surface represents a generalization of the HB criterion through the use of the stress invariants:

$$f = \frac{q^{\frac{1}{a}}}{\sigma_{ci}^{\left(\frac{1}{a-1}\right)}} + A(\theta)\frac{q}{3}m_b - m_b p - s\sigma_{ci} \tag{1}$$

where $p = (\sigma_{xx} + \sigma_{yy} + \sigma_{zz})/3$, $q = \sqrt{1.5(s_{ij}s_{ij})}$, and θ represent the mean stress, the stress deviator, and the Lode angle, respectively. $s_{ij} = \sigma_{ij} - p\delta_{ij}$ is the deviator component of σ_{ij}, δ_{ij} being the Kronecker's symbol whereas the Lode angle is defined through $\cos(3\theta) = \sqrt{6}\, tr(s)^3/tr(s^2)^{3/2}$. Moreover, equation (1) is characterized by the uniaxial compression strength σ_{ci} and the dimensionless HB parameters m_b, s and a. Finally, the generalization of the model for three-dimensional stress states is obtained through the function $A(\theta)$ according to the following expression [13]:

$$A(\theta) = \frac{\cos\left[\frac{\cos^{-1}(k\cos(3\theta))}{3}\right]}{\cos\left[\frac{\cos^{-1}(k)}{3}\right]} \tag{2}$$

where k is a parameter governing the profile of the yield surface in the deviatoric plane, allowing shapes ranging from circular (i.e., k=0) to the one proposed by Jiang and Zhao [14] (i.e., k=-0.9999), as shown in figure 1. Since HBS adopts the yield surface proposed by Jiang [13], the only sharp corners to deal with are those at the intersection between such yield and the isotropic stress cut-off. The classic Koiter-rule [15] for yielding depending on two yield surfaces is used to calculate the different plastic strain rates.

The degradation of the rock mass due to shearing is simulated employing a hyperbolic decreasing of the material properties by considering the following hardening rule:

$$\begin{Bmatrix} m_b \\ s \end{Bmatrix} = \begin{Bmatrix} m_{bi} - \left(\frac{m_{bi}-m_{br}}{B_m - \varepsilon_{eq}^p}\right)\varepsilon_{eq}^p \\ s_i - \left(\frac{s_i - s_r}{B_s - \varepsilon_{eq}^p}\right)\varepsilon_{eq}^p \end{Bmatrix} \tag{3}$$

where subscripts *i* and *r* refer to the initial and residual values of the corresponding variable, whilst ε_{eq}^{p} is the equivalent plastic strain representing the cumulated value of deviatoric plastic strain.

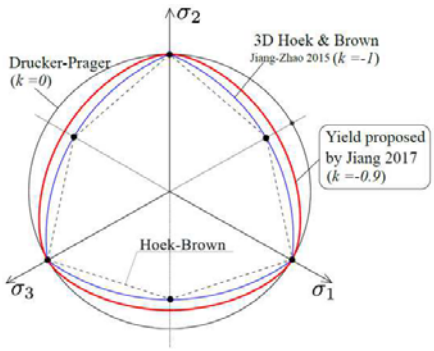

Figure 1. Section of the yield criterion in the deviatoric plane according to the formulation proposed by Jiang [13] (figure rearranged after [13]). Comparison between the original HB and the former yield criterion proposed by the same author [14].

Consistently with the mathematical expression of the yield surface in equation (1), a non-associated plastic flow is introduced in the plastic potential with the variable m_ψ:

$$g = \frac{q^{\frac{1}{a}}}{\sigma_{ci}^{\left(\frac{1}{a-1}\right)}} + A(\theta)\frac{q}{3}m_\psi - m_\psi p \tag{4}$$

The nonlinear trend of dilation is controlled through the same hyperbolic evolution used for the HB parameters [16, 17]:

$$m_\psi = m_{\psi i} - \left(\frac{m_{\psi i} - m_{\psi r}}{B_\psi - \varepsilon_{eq}^{p}}\right)\varepsilon_{eq}^{p} \tag{5}$$

Parameters B_m and B_s in equation (3) govern the rate of softening resulting from the deviatoric shearing, while parameter B_ψ in equation (5) prescribes the rate of dilation after initial yielding.

To introduce a cut-off function in the tensile regime, the mean stress $\bar{p}$ at the apex of the HB envelope is reduced through the parameter α, which ranges between 0 (nil tensile strength) and 1 (no cut-off).

In the brittle/dilatant regime, the development of localized shear bands strongly affects the mesh-objectivity of the response [18]. Therefore, to restore mesh-independency due to strain localization, a visco-plastic regularization is considered based on Perzyna's over-stress theory [19]. To this end, a fluidity parameter γ (figure 2) in conjunction with a temporal gradient is introduced, defining, therefore, an internal scale length controlling the shear band thickness [20].

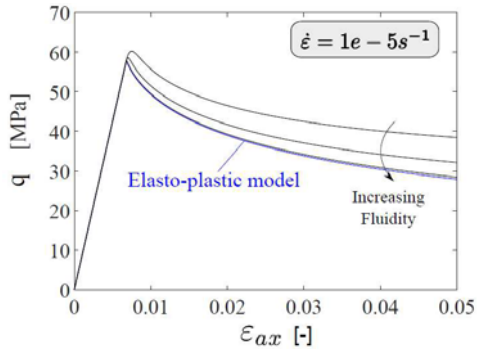

Figure 2. Influence of the fluidity γ on the response of HBS model for a uniaxial compression test and a given loading rate: by increasing the value of the fluidity, the visco-plastic model approaches the elasto-plastic model.

3. Modelling of failure mechanism of rock pillars

Under actual field conditions, the pillar load capacity is reduced to a residual value and failure occurs once the applied stress level exceeds its peak uniaxial compressive strength. HBS is herein adopted for simulating the failure of hard-rock pillars leading to progressive deterioration of pillar strength by

showing that the proposed constitutive model is a potentially powerful tool for the production of engineering designs of rock structures such as mine pillars.

3.1. Material properties and HBS parameters

The material properties used for the analysis are inferred from published data [4] of the Middleton mine (Derbyshire, UK). This mine, whose underground works ceased in 2005, is a classic room-and-pillar mining operation. The orebody consisted of a strong, thickly bedded crystalline limestone whose properties are summarized in table 1 [4].

Table 1. Material properties for the limestone orebody at Middleton mine.

Parameter (intact rock)	**Unit**	**Value**
Unit weight (γ)	kN/m^3	26
Young's modulus (E)	GPa	27
Poisson's ratio (ν)	-	0.3
Uniaxial compressive strength (σ_{ci})	MPa	48
Tensile strength (σ_{ti})	MPa	3.8
Internal cohesion (c_i)	MPa	9
Internal friction (φ_i)	°	45

The HBS parameters adopted for the numerical modelling are reported in table 2. The rock mass parameters have been obtained consistently with the intact rock properties reported in table 1, considering a rock mass characterized by a GSI value equal to 75 [4] and assuming a nil value for the disturbance factor D.

Table 2. Assumed rock mass parameters for HBS constitutive model.

Parameter (rock mass)	**Unit**	**Value**
Young's modulus (E)	GPa	22
Poisson's ratio (ν)	-	0.3
Intact rock compressive strength (σ_{ci})	MPa	48
Tensile strength reduction factor (α)	-	0.3
Geological Strength Index (GSI)	-	75
Intact rock HB parameter (m_i)	-	12
Disturbance factor (D)	-	0
Initial HB parameters (m_{bi} / s_i)	-	4.914 / 0.062
Residual HB parameters (m_{br} / s_r)	-	0.885 / 0.0003
Rate of softening parameters ($B_m = B_s$)	-	0.002
Peak/residual dilation parameter ($m_{\psi i}$ / $m_{\psi r}$)	-	3 / 0
Rate of dilation parameter (B_ψ)	-	0.01
Fluidity (γ)	d^{-1}	15
Shape of yield surface (k)	-	-0.9999

Some additional considerations concerning the proper definition of specific parameters of the HBS model are summarized in what follows:

- the residual strength parameters have been inferred from a residual GSI obtained following the approach suggested by Cai et al. [21];
- the peak dilation parameter is based on the rock mass dilation angle definition as a function of GSI and intact rock friction angle proposed by Alejano et al. [22];

- the rate of softening parameters (defining the strain level range for peak/residual strength transition) has been calibrated based on stress-strain responses of Middleton pillar models reported in Elmo and Stead [4];
- the fluidity parameter has been calibrated so that the rate-dependency of the regularization effect is minimal (figure 2).

3.2. Numerical analysis with HBS model

The initial series of analyses are aimed at showing the progressive pillar failure having different width-to-height (*w*/*h*) ratios. Conceptual 2D models of pillars 7 m high have been simulated with the loading being applied via prescribed displacements as if they were subjected to uniaxial loading conditions in servo-controlled laboratory tests. Figure 3 and figure 4 report the results showing the through-going shear bands developed once residual strength is approached and the corresponding stress-strain curves, respectively. The shear bands represent the actual generation of shear fractures in the field, resulting from the coalescence of the cracks induced during the fracturing process. The plot of the failed zones within the pillar (figure 3) highlights the development of deteriorated pillar hourglassings. It is evident that slender pillars (low *w*/*h* ratio) behave in a more brittle fashion than squat pillars (high *w*/*h* ratio), where the degradation process is associated with strain-softening of the pillar (figure 4). A more marked loss of load-carrying capability related to the generation of thick and neat shear fractures into the core of the pillar is observed for slender pillars. In contrast, a significant increase in capacity is shown by heavily fractured squat pillars and where failure is due to small through-going fractures.

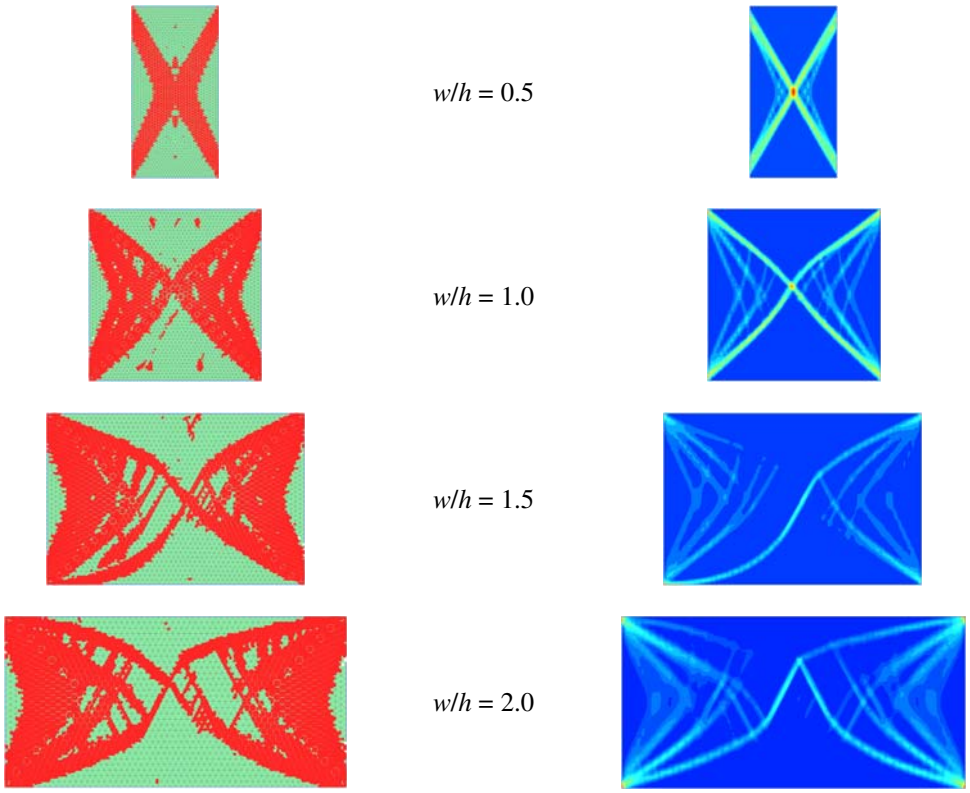

Figure 3. Failure of pillars with different *w*/*h* ratios: stress points in plastic conditions (left) and corresponding deviatoric strain contour (right).

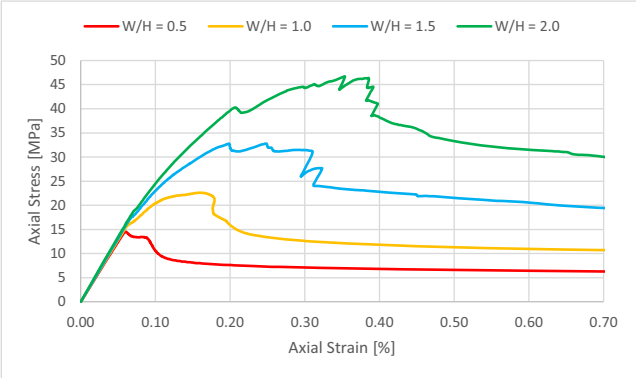

Figure 4. Stress-strain profile for pillars with different *w*/*h* ratios.

These results are in agreement with available predictions carried out with different modelling approaches [e.g., 3, 4]. Moreover, by using the empirical formula proposed by Lunder and Pakalnis [23] for assessing the same pillar, strengths of 14.9 MPa, 20.3 MPa, and 29.4 MPa would be obtained for w/h equal to 0.5, 1, and 2, respectively, confirming how empirical formulae may be over-conservative for pillars with $w/h \geq 2$ [e.g., 1, 3].

Additional numerical analyses have also been carried out to show how these considerations on the pillar-failure mechanism are paramount for designing mine pillars system subjected to high in-situ stress conditions that can potentially cause the hard rock to fail. Since the actual cover of the Middleton mine was about 100 m, a greater depth equal to 500 m has been assumed to generate high in-situ stresses for the scope of the current study. Figure 5 shows the adopted model geometry representing the mine pillar located between two rooms 14 m wide subjected to in-situ conditions characterized by a vertical stress σ_v of 13 MPa and a stress ratio K_0 of 0.5. The model is then used to examine pillars of 3.5, 7, 10.5, 14 m wide x 7 m high (aspect ratio *w*/*h* ranging from 0.5 to 2).

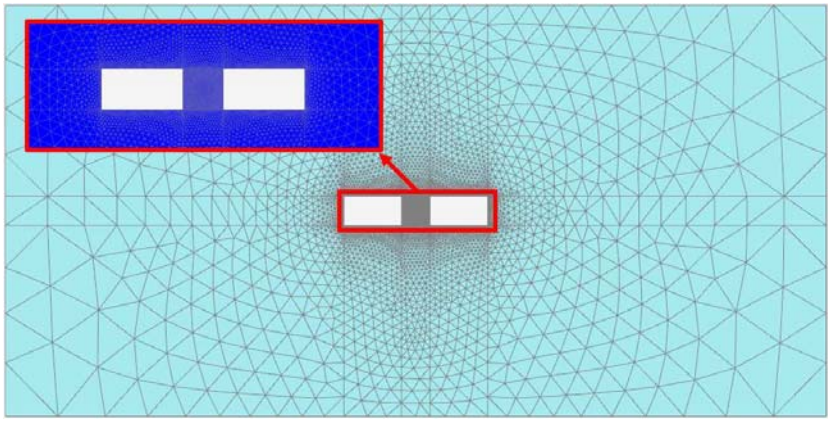

Figure 5. Detail of model geometry.

The results reported in figure 6 show that, under these field conditions, the development of through-going shear fractures, indicating loss of load-carrying capacity, occurs for lower *w*/*h* ratios (0.5 and 1). On the other hand, for a higher *w*/*h* ratio (1.5 and 2), induced cracks coalesce to form shear bands in the pillar sidewalls with the development of pillar hourglassing. In the latter case, limited progressive fracturing and lateral spalling occur, likely involving displacements of large blocks, albeit overall without compromising the bearing capacity of the pillar.

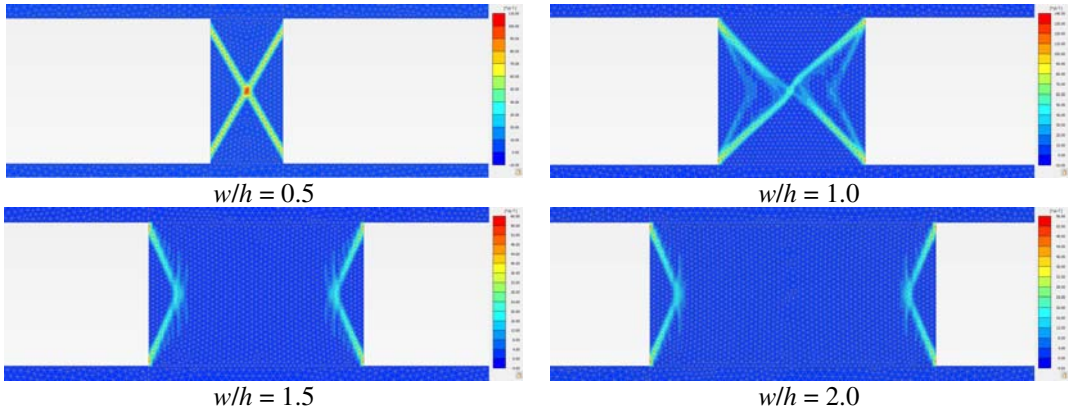

Figure 6. Failure of pillars with different *w*/*h* ratios: shear bands identified

4. Conclusions

Brittle failure around underground openings involves spalling and slabbing leading to the degradation of the surrounding rock mass. Understanding such progressive brittle failure behaviour is essential for the design of rock pillars. This paper has investigated the use of the HBS model implemented in the commercial FEM code PLAXIS to model mine pillars' failure process.

To assess the performance of the HBS model in capturing the progressive failure, the first set of analyses has been performed on conceptual 2D models of pillars subjected to uniaxial loading conditions. As a result, it is shown how the proposed constitutive approach allows the simulation of shear fractures resulting from the coalescence of the induced cracks as a consequence of the rock mass degradation. The HBS model confirms the prediction of the increase of the pillar strength as well as the transition from brittle to strain-softening behaviour with an increasing pillar aspect ratio.

Furthermore, the constitutive model has been employed to simulate the mine pillars system behaviour in an underground mining operations environment. The analysis of pillars behaviour under actual field conditions has shown the capability of the HBS model to properly simulate the behaviour of rock pillars at the high-stress levels associated with deep mining conditions and thus the suitability of the constitutive approach as a tool for an improved and effective production of engineering design for the sizing of rock pillars.

References

[1] Martin C D and Maybee W G 2000 The strength of hard-rock pillars *Int J Rock Mech Min Sci* **37**:1239-1246

[2] Diederichs M S, Coulson A, Falmagne V, Rizkalla M and Simser B 2002 Applications of rock damage limits to pillar analysis at Brunswick *Mine Mining and tunnelling innovation and opportunity: Proc. of the 5th North American Rock Mechanics Symp. and 17th Tunnelling Association of Canada Conf.*, eds Hammah R, Bawden W, Curran J, and Telesnicki M Toronto, Ontario, University of Toronto Press

[3] Fang Z and Harrison J P 2002 Numerical analysis of progressive fracture and associated behaviour of mine pillars by use of a local degradation model *Trans Inst Min Metall* **111**:A59–A72

[4] Elmo D and Stead D 2010 An integrated numerical modelling–discrete fracture network approach applied to the characterisation of rock mass strength of naturally fractured pillars *Rock Mech Rock Eng* **43**(1):3–19

[5] Wang S Y, Sloan S W, Huang M L and Tang C A 2011 Numerical study of failure mechanism of serial and parallel rock pillars *Rock Mech Rock Eng* **44**:179–198

[6] Rafiei Renani H and Martin C D 2018 Modeling the progressive failure of hard rock pillars *Tunnelling and Underground Space Technology* **74**:71-81
[7] Hajiabdolmajid V Kaiser P K and Martin C D 2002 Modelling brittle failure of rock *Int J Rock Mech Min Sci* **39**(6):731–41.
[8] Fang Z and Harrison J P 2002 Development of a local degradation approach to the modelling of brittle fracture in heterogeneous rocks *Int J Rock Mech Min Sci* **39**:443–457.
[9] Diederichs M S 2007 The 2003 Canadian Geotechnical Colloquium: mechanistic interpretation and practical application of damage and spalling prediction criteria for deep tunnelling. *Canadian Geotechnical Journal* **44**(9):1082–116.
[10] Marinelli F, Zalamea N, Vilhar G, Brasile S, Cammarata G and Brinkgreve R 2019 Modeling of brittle failure based on Hoek & Brown yield criterion: parametric studies and constitutive validation *Proc. of 53rd US Rock Mech/Geomech Symp.*, New York, 23-26 June 2019. Paper 19–410
[11] Plaxis bv, Bentley Systems Inc. 2021 *PLAXIS 2D Manuals* Connect Edition V22.01
[12] Zalamea N, Marinelli F, Cammarata G, Brinkgreve R and Brasile S 2020 Numerical analyses of shear bands failure in tunnel excavation problems using a regularized Hoek-Brown model. In *Proc. of 53rd US Rock Mech/Geomech Symp.*, Golden, Colorado 28 June – 1 July 2020. Paper 20–1797
[13] Jiang H 2017 A failure criterion for rocks and concrete based on the Hoek-Brown criterion *Int J Rock Mech Min Sci* **95**:62–72
[14] Jiang H and Zhao J 2015 A simple three-dimensional failure criterion for rocks based on the Hoek-Brown criterion. *Rock Mech Rock Eng* **48**(5):1807–1819
[15] Koiter W T 1960 General theorems for elastic plastic solids *Progress of solid mechanics*, eds. JN Sneddon and R Hill (Noth Holland, Amsterdam) pp 167-221.
[16] El Moustapha K 2014 Identification de lois de comportement enrichies pour les géomatériaux en présence d'une localisation de la déformation *PhD Thesis* Université de Grenoble, Laboratoire 3SR, Equipe GDR, France.
[17] Fatemeh S, Collin F, and Charlier R 2017 On the variable dilatancy angle in rocks around underground galleries *Rock Mech Rock Eng* **50**:587–60
[18] Pijaudier-Cabot G and Bazant Z P 1987 Nonlocal damage theory *J Engineering Mech ASCE* **113**:1512–1533
[19] Perzyna P 1966 Fundamental problems in viscoplasticity *Advances in Applied Mechanics* **9**:243-377.
[20] Sluys L J 1994 Wave propagation, localization and dispersion in softening solids *Ph.D. Thesis* Delft University of Technology, The Netherlands.
[21] Cai M, Kaiser P K, Tasaka Y and Minami M 2007 Determination of residual strength parameters of jointed rock masses using the GSI system *Int J Rock Mech Min Sci* **44**(2):247–265
[22] Alejano L, Alonso E, Rodríguez-Dono A and Fernández-Manín G 2010 Application of the convergence-confinement method to tunnels in rock masses exhibiting hoek-brown strain softening behaviour *Int J Rock Mech Min Sci* **47**(1):150-160.
[23] Lunder P J, Pakalnis R 1997 Determination of the strength of hard-rock mine pillars *Bull Can Inst Min Metall* **90**:51–55